

Correlation effects in the low-energy region of nickel photoemission spectra

F. Manghi and V. Bellini*

Istituto Nazionale per la Fisica della Materia and Dipartimento di Fisica, Università di Modena, Via Campi 213/a, I-41100 Modena, Italy

J. Osterwalder and T. J. Kreutz

Physik-Institut, Universität Zürich, Winterthurerstrasse 190, CH-8057 Zürich, Switzerland

P. Aebi

Institut de Physique, Université de Fribourg, Pérolles, CH-1700 Fribourg, Switzerland

C. Arcangeli

Max-Planck-Institut für Festkörperforschung, Heisenbergstrasse 1, D-70569 Stuttgart, Germany

The role of on-site correlation in the low-energy excitations of nickel is studied by comparing the results of high-angular and high-energy resolution photoemission spectroscopy with quasiparticle states calculated as a three-body scattering solution of a multiorbital Hubbard model. It is found that correlation effects modify the energy dispersion and spin polarization of electron states and are essential in order to get a quantitative agreement with experimental data.

It is well established that the photoemission spectra of narrow-band materials, such as the elements of the d transition-metal series and their compounds, cannot be entirely explained within a one-electron picture, due to the presence of local correlations between electrons in the partially filled d band.¹ Band mapping, i.e., the reduction of the measured spectra to a band structure and its comparison with theoretical results can be a powerful tool to directly investigate correlation effects, provided that some important requirements are fulfilled: on the experimental side, high-angular and high-energy resolution photoemission techniques are necessary in order to identify quasiparticle energy dispersions and lifetime broadenings associated with the many-body character of the electronic excitations; on the theoretical side, a realistic description of the band structure must be combined with an accurate treatment of many-body electron-electron interactions to account for the mixed itinerant and localized behavior of the valence states.

In this paper we present direct evidence of correlation effects in the low binding-energy region of the valence band of nickel. While these effects dominate the high-energy region of the Ni photoemission spectrum with the presence of the well-known 6 eV satellite peak,² the electron states near the Fermi energy are commonly believed to be less influenced by many-body interactions; this has to do with the very general properties of low-energy excitations of Fermi liquids,³ but also with the observation that the Fermi surface of ferromagnetic nickel is nicely reproduced by a single-particle band structure.⁴ All the same, significant discrepancies are known to exist between the observed energy dispersions of some bands and the results of standard single-particle band calculations;⁵ these discrepancies are related to the energy renormalization due to electron-electron interaction. Here we want to investigate these effects in detail in order to get a band mapping of low-energy quasiparticle excitations.

A high-resolution photoemission data set was measured at room temperature on a Ni(110) surface. Using He I radiation for excitation ($h\nu = 21.21$ eV), energy spectra were taken in 1° steps for a continuous range of polar angles along the (001) plane, from normal emission ($\theta_m = 0^\circ$) to a polar angle of $\theta_m = 70^\circ$ off normal. Each spectrum spans a binding-energy range from -300 meV (above E_F) to 1200 meV (below E_F) and was measured with an energy resolution of 35 meV. The angular resolution was set to $\pm 0.5^\circ$ using an iris aperture in front of the entrance lens to the hemispherical analyzer. Further details on the experimental procedure and on the particular region in reciprocal space probed by these spectra have been given elsewhere.⁶

On the theoretical side we have calculated spectral functions and quasiparticle energies by solving a multiorbital Hubbard Hamiltonian according to the three-body scattering (3BS) method.⁷⁻¹¹ This approach can be seen as an extension to the solid state of the configuration-interaction scheme used for finite systems: the Hubbard Hamiltonian is projected on a set of states obtained by adding a finite number of electron-hole pairs to the ground state of the single-particle Hamiltonian and this expansion is truncated to include one electron-hole pair; this approximation is particularly justified for systems with a large band occupation since the role of extra configurations depends on the overall number of empty states necessary for the addition of electron-hole pairs.

The effect of electron correlation on one-electron removal energies from a partially filled band is described in terms of interactions between three-body configurations (one hole plus one electron-hole pair) giving rise to hole-hole and hole-electron scattering; the efficiency of these scattering processes depends first of all on the strength of the screened on-site electron-electron interaction, that is on the Coulomb and exchange integrals $U_{\alpha\beta}$ and $J_{\alpha\beta}$: $U_{\alpha\beta}$ describes the Coulomb repulsion among opposite spin electrons on the

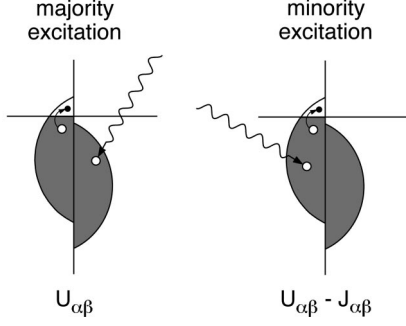


FIG. 1. Schematic representation of the interactions involved in the photoemission from majority- and minority-spin bands.

same site belonging to orbitals α and β , and $U_{\alpha\beta} - J_{\alpha\beta}$ the interactions among parallel spin ones.

The scattering efficiency depends also on the number of empty d states necessary for the creation of three-particle configurations since no electron-hole pair can be added to a completely filled band: in the case of nickel where only the minority-spin band has a sizable number of empty states available the creation of a majority-spin hole will be followed by scattering processes involving only opposite spin electron-hole pairs—of intensity proportional to $U_{\alpha\beta}$ —while the creation of a minority-spin hole will involve less intense scattering of strength proportional to $U_{\alpha\beta} - J_{\alpha\beta}$ with parallel spin electron-hole pairs only (Fig. 1). For this reason self-energy renormalization will affect spin-up states more strongly than spin-down ones.

The interactions between the three-body configurations are represented by a set of scattering T -matrices $T_{h-h}^{\alpha\beta}$ and $T_{h-e}^{\alpha\beta}$, describing hole-hole and electron-hole scattering, respectively. For a majority-spin hole we have

$$T_{h-h}^{\alpha\beta}(\omega) = \frac{U_{\alpha\beta}}{1 + U_{\alpha\beta}g_3^{\alpha\beta}(\omega)}, \quad (1a)$$

$$T_{h-e}^{\alpha\beta}(\omega) = \frac{-U_{\alpha\beta}}{1 - U_{\alpha\beta}g_1^{\alpha\beta}(\omega)}, \quad (1b)$$

with

$$g_3^{\alpha\beta}(\omega) = \int_{-\infty}^{E_f} d\epsilon' \int_{-\infty}^{E_f} d\epsilon \frac{n_{\alpha-\sigma}(\epsilon)n_{\beta\sigma}(\epsilon')}{\omega - \epsilon' - \epsilon - i\delta}, \quad (2a)$$

$$g_1^{\alpha\beta}(\omega) = \int_{-\infty}^{E_f} d\epsilon' \int_{E_f}^{\infty} d\epsilon \frac{n_{\alpha-\sigma}(\epsilon)n_{\beta\sigma}(\epsilon')}{\omega - \epsilon' + \epsilon - i\delta}, \quad (2b)$$

$n_{\alpha\sigma}(\epsilon)$ is the spin-dependent orbital density of d single-particle valence states

$$n_{\alpha\sigma}(\epsilon) = \sum_{\mathbf{k}n} |C_{\alpha\sigma}^n(\mathbf{k})|^2 \delta(\epsilon - \epsilon_{\mathbf{k}}^n),$$

where $C_{\alpha\sigma}^n(\mathbf{k})$ are the expansion coefficients of Bloch single-particle states in terms of localized orbitals. The Faddeev theory¹² is used to determine the total scattering matrix and the resolvent of the many-body system. The hole self-energy is given by

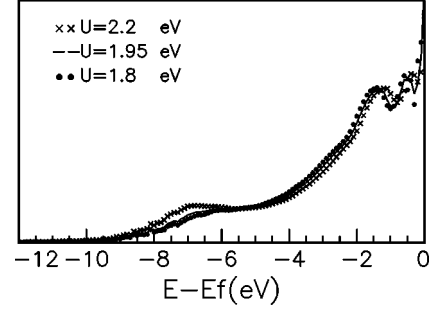


FIG. 2. Density of quasiparticle states of nickel for majority-spin states calculated with $U_{dd}=2.2$ eV (crosses), $U_{dd}=1.95$ eV (continuous line), and $U_{dd}=1.8$ eV (dots).

$$\Sigma_{\mathbf{k}n\sigma}^-(\omega) = \sum_{\beta} |C_{\beta\sigma}^n(\mathbf{k})|^2 \left[\sum_{\alpha} U_{\alpha\beta} \frac{1}{N} \sum_{\mathbf{k}'n'}^{\text{empty}} |C_{\alpha-\sigma}^{n'}(\mathbf{k}')|^2 - \Sigma_{\beta\sigma}^-(\omega) \right], \quad (3)$$

where

$$\Sigma_{\beta\sigma}^-(\omega) = \sum_{\alpha} \int_{E_f}^{\infty} d\epsilon n_{\alpha-\sigma}(\epsilon) T_{h-h}^{\alpha\beta}(\omega - \epsilon) \times [1 + U_{\alpha\beta}A^{\alpha\beta}(\omega - \epsilon)]. \quad (4)$$

$A^{\alpha\beta}$ is the quantity related to $T_{h-e}^{\alpha\beta}$ and is determined by a numerical solution of the integral equation described in Ref. 10. The analysis is the same for the addition of one minority-spin hole, the only differences being $U_{\alpha\beta} - J_{\alpha\beta}$ instead of $U_{\alpha\beta}$ to describe interactions among parallel spin particles and the substitution $-\sigma \rightarrow \sigma$ in Eqs. (1)–(4).

The key quantity to be compared with photoemission spectra is the hole spectral function

$$D_{\mathbf{k}n\sigma}^-(\omega) = -\frac{1}{\pi} \text{Im} \frac{1}{\omega - \epsilon_{\mathbf{k}n\sigma} - \Sigma_{\mathbf{k}n\sigma}^-(\omega)}$$

describing the response of the system to the removal of an electron of momentum \mathbf{k} and spin σ .

The calculation of self-energy corrections and spectral functions requires as an input (i) the band structure (eigenvalues, eigenvectors, and orbital density of states) and (ii) the values of the Coulomb and exchange parameters. The band structure of ferromagnetic nickel has been calculated with the linear muffin-tin orbital (LMTO) method in the atomic-spheres approximation including the combined correction term.¹³ The tight-binding LMTO basis set¹⁴ has been used, including nine orbitals (s , p , and d) per atom. The Coulomb and exchange parameters have been fixed to reproduce the observed energy position of the valence-band satellite. In particular we have chosen $U_{\alpha\beta} = U_{dd} = 1.95$ eV and $J_{\alpha\beta} = J_{dd} = 0.5$ eV. Values of U_{dd} in the range 2.2–1.8 eV do not affect appreciably the energy position of the 6 eV satellite (see Fig. 2) and are in agreement with current estimates;^{15,16} the present choice optimizes the agreement between theory and experiments in the low-energy region of the spectra as well.

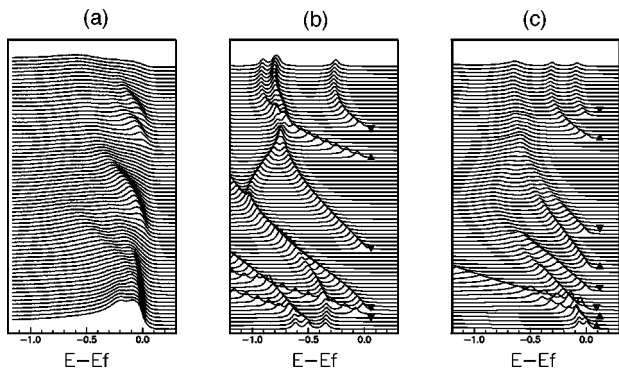


FIG. 3. Comparison between angle-resolved photoemission spectra (a), single particle local-density approximation (LDA) (b), and quasiparticle 3BS (c) results. The polar angle ranges from 0° (bottom) to 70° (top). The spin character is indicated by \blacktriangle and \blacktriangledown .

In Fig. 3 we focus onto the energy region of a few hundred meV below the Fermi energy. The results of the angle-resolved photoemission experiment are compared with theoretical spectral functions. The measured polar angle ranges from 0° to 70° and the sampled k vectors have been calculated to match those of the experimental data assuming an inner potential of 10.7 eV and a work function of 4.7 eV.⁴

Figure 3(a) shows the raw experimental data as a quasi-continuous series of energy spectra. The intensity drop at E_F is clearly visible in all spectra. One can well distinguish two bands crossing the Fermi level between $\theta_m = 50^\circ$ and 60° ; they have been identified as an exchange-split sp band closely related to the Σ_1 band.⁶ Between $\theta_m = 20^\circ$ and 30° a single band is observed, associated with the $\Sigma_{1/2}$ band in the minority channel. Finally, the region between $\theta_m = 20^\circ$ and normal emission is crowded with bands near the Fermi energy, with at least three different bands converging very close to E_F for $\theta_m = 0^\circ$. Here, states near the X point of the Brillouin zone are probed.⁶

Figures. 3(b) and 3(c) show the spectral functions D_σ^-

obtained within the single-particle picture and including self-energy corrections, respectively. The inclusion of correlation effects strongly modifies the spectra: all the structures are pushed up towards E_f by self-energy corrections reproducing much more closely the experimental results both in terms of energy position and dispersion.

We want to stress here some basic issues that turned out to be very important in order to obtain a quantitative comparison between theory and experiments: as already mentioned and discussed in detail in a previous paper,¹⁰ the self-energy is, in the present 3BS approach, a k -vector-, energy-, and spin-dependent complex function [see Eq. (4)]. The k dependence in particular is essential in order to reproduce the energy dispersion observed experimentally since the single-particle results are inadequate both in terms of energy positions and dispersions. The present approach fully includes the hybridization between sp and d states accounted for by first-principles band theory. The self-energy turns out to be k dependent, depending on the weight of the d orbital contribution, and band states at different k points are thus differently shifted.

The spin dependence of the self-energy, arising from the different efficiencies of the scattering channels involving majority- and minority-spin electrons, strongly affects the spin polarization of the quasiparticle states as it appears quite clearly in Fig. 3. For this particular region in k space, four spin-up and four spin-down bands are theoretically predicted in the energy region of interest. While in the single-particle picture one spin-up band and four spin-down bands cross the Fermi energy, all four spin-up bands come close to E_F after the inclusion of correlation effects. Moreover, the energy separation between the spin-up and spin-down bands between $\theta_m = 50^\circ$ and 60° is reduced by self-energy corrections. All this is in excellent agreement with the experimental data.

The role of correlation in improving the agreement between theory and experiments appears even more clearly in

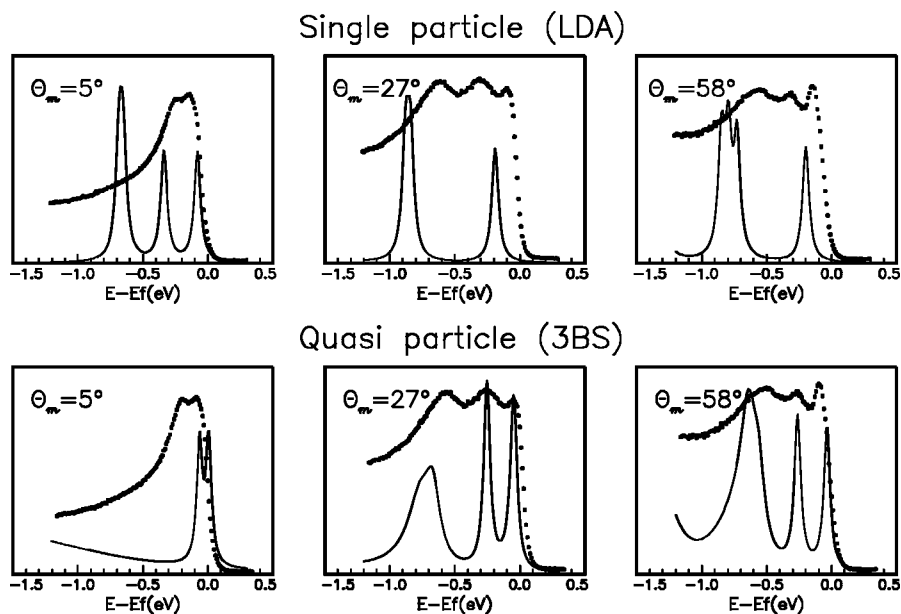


FIG. 4. Comparison between k -resolved photoemission spectra (dots) and theoretical spectral function (continuous line) calculated according to single-particle LDA and quasiparticle 3BS approaches. The k points correspond to the reported values of the polar angle θ_m .

TABLE I. Values of polar angles θ_m where bands cross the Fermi level.

	Expt.	LDA	QP (3BS)
Σ_1^\downarrow	54.5°	52.5°	55.5°
Σ_1^\uparrow	49.5°	44.5°	49.5°
Σ_2^\downarrow	27.0°	20.5°	24.5°

Fig. 4, where experimental curves, single-particle and quasiparticle (3BS) spectral functions are compared at some particular k points. From this figure it is obvious that the quasiparticle spectral functions provide a rather accurate description of the measured photoemission data, with some shifts in the order of 150 meV remaining for the d -band excitation near 600 meV binding energy. The single-particle calculations, on the other hand, fail completely to describe the data. As expected, this failure is less pronounced as regards to the angular positions of the Fermi-level crossings, i.e., the shape and the volume of the Fermi surface.^{3,4} Nevertheless, Table I shows that the quasiparticle Fermi-level crossings are in all measurable cases closer to the experimental ones by a significant amount.

Finally, since the calculated self-energy is a complex function with both a real *and* an imaginary part the resulting

quasiparticle states have intrinsic, finite lifetimes. This is not the case when other approximate forms of either the self-energy¹¹ or of the Green's function¹⁷ are adopted. A quantitative analysis of linewidths is, however, beyond the aim of the present paper since it would require a full treatment of both photoelectron and photohole lifetimes.¹⁸

The main approximation of the present theoretical approach is related to the truncated configuration expansion including up to three particles (one hole plus one e-h pair); for the particular case of nickel, due to the small number of empty d states, configurations with more than one e-h pair are expected to play a minor role.¹⁰

In conclusion, we have shown that on-site correlations that are known to affect the high binding-energy region of the valence spectrum of nickel, modify also the low-energy excitations. The inclusion of realistic band-structure eigenvalues and an accurate treatment of many-body interactions are essential in order to obtain a theoretical description of the electron states near the Fermi surface in quantitative agreement with high-angular and high-energy resolution photoemission data.

This work has been supported by the Swiss National Science Foundation and has benefited from the collaboration within the ESF Program on ‘‘Electronic Structure Calculations for Elucidating the Complex Atomistic Behavior of Solids and Surfaces.’’

*Present address: Institut fuer Festkoerperforschung Forschungszentrum, D-52425 Juelich, Germany.

¹*Angle-Resolved Photoemission*, edited by S. D. Kevan (Elsevier, Amsterdam, 1992).

²C. Guillot, Y. Ballu, J. Pagné, J. Lecante, K. Jain, P. Thiry, R. Pinchaux, Y. Pétrouff, and L.M. Falicov, Phys. Rev. Lett. **39**, 1632 (1977).

³J.M. Luttinger, Phys. Rev. **121**, 942 (1961).

⁴P. Aebi, T.J. Kreutz, J. Osterwalder, R. Fasel, P. Schwaller, and L. Schlapbach, Phys. Rev. Lett. **76**, 1150 (1996).

⁵W. Eberhardt and E.W. Plummer, Phys. Rev. B **21**, 3245 (1980).

⁶T.J. Kreutz, P. Aebi, and J. Osterwalder, Solid State Commun. **96**, 339 (1995).

⁷J. Igarashi, J. Phys. Soc. Jpn. **52**, 2827 (1983); **54**, 260 (1985).

⁸C. Calandra and F. Manghi, Phys. Rev. B **50**, 2061 (1994).

⁹F. Manghi, C. Calandra, and S. Ossicini, Phys. Rev. Lett. **73**, 3129 (1994).

¹⁰F. Manghi, V. Bellini, and C. Arcangeli, Phys. Rev. B **56**, 7149 (1997).

¹¹Jun-ichi Igarashi, P. Unger, K. Hirai, and P. Fulde, Phys. Rev. B **49**, 16 181 (1994).

¹²L.D. Faddeev, Zh. Éksp. Teor. Fiz. **39**, 1459 1960 [Sov. Phys. JETP **12**, 1014 (1961)].

¹³O.K. Andersen, Phys. Rev. B **12**, 3060 (1975).

¹⁴O.K. Andersen and O. Jepsen, Phys. Rev. Lett. **53**, 2571 (1984).

¹⁵M.M. Steiner, R.C. Albers, and L.J. Sham, Phys. Rev. B **45**, 13 272 (1992).

¹⁶M. Springer and F. Aryasetiawan, Phys. Rev. B **57**, 4364 (1998).

¹⁷W. Borgiel and W. Nolting, Z. Phys. B **78**, 241 (1989).

¹⁸N.V. Smith, P. Thiry, and Y. Petroff, Phys. Rev. B **47**, 15 476 (1993).